Journal of Traditional and Complementary Medicine 14 (2024) 391–402

Contents lists available at ScienceDirect

Journal of Traditional and Complementary Medicine

journal homepage: www.elsevier.com/locate/jtcme

Red rice bran aqueous extract ameliorate diabetic status by inhibiting intestinal glucose transport in high fat diet/STZ-induced diabetic rats

Atcharaporn Ontawong [a,*], Sirinat Pengnet [a], Arthid Thim-Uam [b], Chutima S. Vaddhanaphuti [c], Narongsuk Munkong [d], Manussaborn Phatsara [e], Kullanat Kuntakhut [f], Jakkapong Inchai [c], Doungporn Amornlerdpison [f,g], Teerawat Rattanaphot [f]

[a] Division of Physiology, School of Medical Sciences, University of Phayao, 19 Moo 2 Mae-Ka District, Muang, Phayao, 56000, Thailand
[b] Division of Biochemistry, School of Medical Sciences, University of Phayao, 19 Moo 2 Mae-Ka District, Muang, Phayao, 56000, Thailand
[c] Faculty of Medicine, Chiang Mai University, 110 Faculty of Medicine, CMU, Inthawarorot Rd., Sri Phum, Muang, Chiang Mai, 50200, Thailand
[d] Department of Pathology, School of Medicine, University of Phayao, 19 Moo 2 Mae-Ka District, Muang, Phayao, 56000, Thailand
[e] Department of Anatomy, Faculty of Medicine, Chiang Mai University, Chiang Mai, 52000, Thailand
[f] Center of Excellence in Agricultural Innovation for Graduate Entrepreneur, Maejo University, 63, Sansai-Phrao Street, Sansai, Chiang Mai, 50290, Thailand
[g] Faculty of Fisheries Technology and Aquatic Resources, Maejo University, Chiang Mai, 50290, Thailand

ARTICLE INFO

Keywords:
Diabetes mellitus
Red rice bran aqueous extract
Glucose transporter 2 (GLUT2)
Glucose uptake
Sodium-dependent glucose cotransporter 1 (SGLT1)

ABSTRACT

Red rice (*Oryza sativa* L.) consumption has grown recently, partly due to its potential health benefits in several disease prevention. The impact of red rice bran aqueous extract (RRBE) on intestinal glucose uptake and diabetes mellitus (DM) progression has not been thoroughly investigated. This study aimed to evaluate the effect of RRBE on *ex vivo* intestinal glucose absorption and its potential as an antihyperglycemic compound using a high-fat diet and streptozotocin (STZ)-induced diabetic rats. High-fat diet/STZ-induced diabetic rats were supplemented with either 1000 mg/kg body weight (BW) of RRBE, 70 mg/kg BW of metformin (Met), or a combination of RRBE and Met for 3 months. Plasma parameters, intestinal glucose transport, morphology, liver and soleus muscle glycogen accumulation were assessed. Treatment with RRBE, metformin, or combination markedly reversed hyperglycemia, hypertriglyceridemia, insulin resistance, and pancreatic morphology changes associated with T2DM. Correspondingly, all supplements effectively downregulated glucose transporters, resulting in a reduction of intestinal glucose transport—additionally, liver and soleus muscle glycogen accumulation was reduced in RRBE + Met treated group. Taken together, RRBE potentially suppressed intestinal glucose transporters' function and expression, reducing diabetic status.

1. Introduction

Glucose is a primary energy source for both aerobic and anaerobic cellular respiration. Glucose from foods is absorbed across the absorptive enterocytes of the small intestine. The glucose is transported across the brush border membrane (BBM) to the bloodstream through a sodium-dependent glucose cotransporter 1 (SGLT1). In addition, glucose is transferred from the blood flow via glucose transporter 2 (GLUT2) localized in the basolateral membrane.[1–3] A previous study reported that 2 h after eating a meal in humans, glucose was found in the upper intestinal tract.[4] The main point is that the intestinal barrier plays a role in blood glucose level control. Therefore, any change in these transporters will likely affect blood glucose levels. The increment of intestinal SGLT1 and GLUT2 expression and function is involved in hyperglycemia and diabetes mellitus.[1] Hyperglycemia is a hallmark of type 2 diabetes (T2DM), diagnosed when fasting blood sugar exceeds 126 mg/dL. A significant level of intestinal glucose uptake in diabetic conditions relates to small intestinal SGLT1 and GLUT2 expression.[5–8] Therefore, it is reasonable to consider these transporters as targets for treating T2DM.

Rice is a significant grain consumed by the world's population. Asia-

Peer review under responsibility of The Center for Food and Biomolecules, National Taiwan University.

* Corresponding author. Division of Physiology, School of Medicals Sciences, University of Phayao 19 Moo 2 Mae-Ka District, Muang, Phayao, 56000, Thailand.
E-mail addresses: atcharaporn.on@up.ac.th (A. Ontawong), sirinat.pe@up.ac.th (S. Pengnet), arthidth@gmail.com (A. Thim-Uam), chutima.srimaroeng@cmu.ac.th (C.S. Vaddhanaphuti), jittmunkong@gmail.com (N. Munkong), kullanat.ktk@gmail.com (K. Kuntakhut), jakkapong.inc@gmail.com (J. Inchai), doungpornfishtech@gmail.com (D. Amornlerdpison), meenakornyong@gmail.com (T. Rattanaphot).

https://doi.org/10.1016/j.jtcme.2023.12.003
Received 21 July 2023; Received in revised form 14 November 2023; Accepted 24 December 2023
Available online 25 December 2023

Pacific is the world's central rice-growing region. It has an output of approximately 90 % of the world's total production. Some byproducts occur in the rice milling process, including 20 % of the rice husk, germ, and seed coat, known as rice bran, and 10.5 % of whole-grain rice. However, some studies indicate that excessive white rice consumption increases the risk of diabetes or metabolic syndrome.[9,10] Thus, colored rice is widely consumed by health-conscious and older consumers. The red, purple, and black rice bran has several advantageous effects, such as anti-cancer, anti-inflammatory, and antioxidant properties. However, different bran colors contain different pigments and major components. Previous studies reported that red rice contains several active compounds, including proanthocyanidin, catechin, epicatechin, 3-*O*-gallates, and epigallates.[11,12] Red rice crude extract has anti-cancer, anti-inflammatory, antioxidant properties, anti-obesity, and improved insulin resistance.[13–16] Furthermore, red rice bran extract has anti-cancer properties by inhibiting cancer cell growth.[17,18] It was also found that ethanol extract from red jasmine rice bran had the best antioxidant activity compared to other strains.[19] The red rice bran extract also shows anti-obesity activity by reducing glucose transport into fat cells 3T3-L1 via α-glucosidase and α-amylase enzyme inhibition compared with purple rice bran extract.[19] A recent study demonstrated that red rice bran ethanol extract modulates liver and skeletal muscle glucose transporter 4 (GLUT4), skeletal muscle insulin-degrading enzyme expression resulting in decreased insulin resistance in obese mice.[14] However, the effect of red rice bran aqueous extract on glucose transport through intestinal epithelium cells in diabetic condition remain unclear. Therefore, the possibility of a protective effect of RRBE on intestinal glucose transporter function, as well as potential mechanisms, are addressed in this study on experimental T2DM rats.

The findings provide insight into the possible advantages of RRBE supplementation in diabetes mellitus and associated conditions.

2. Materials and methods

2.1. Chemicals

Streptozotocin and CelLytic™ mammalian tissue lysis/extraction reagents were purchased from Sigma Aldrich (St. Louis, MO, USA). Polyclonal rabbit anti-SGLT1, GLUT2, 5′ AMP-activated protein kinase, and p-AMPK were purchased from Merck KGaA. Monoclonal mouse alkaline phosphatase (ALP) antibodies were obtained from Novus Biologicals, LLC. Monoclonal mouse anti-β-actin and hepatocyte nuclear factor 1 alpha (HNF1α) were purchased from Abcam. 2-(N-(7-nitrobenz-2-oxa-1,3-diazol-4-yl)amino)-2-deoxyglucose (2-NBDG) was obtained from Thermo Fisher Scientific, Inc. All other chemicals with high purity were obtained from commercial sources.

2.2. Red rice bran aqueous extract preparation, qualification, total phenolic and anthocyanin content measurement

Red glutinous rice bran was purchased from a Thai farmer at Ban Dok Bua, Ban Tun sub-district, Muang Phayao district, Phayao, Thailand. A hundred grams of dried red rice bran (RRB) was boiled in 1000 mL water at 100 °C for 10 min. RRB aqueous solution was filtered through filter paper before being freeze-dried using a freeze dryer (Scanvac, Lillerød, Denmark), producing RRBE with a yield of 20 % (w/w). The chemical constituents of RRBE, namely epicatechin, protocatechuic acid, vanillic acid, caffeic acid, and chlorogenic acid (Sigma-Aldrich; St. Louis, MO, USA), were utilized as benchmarks for validation and quantification through high-performance liquid chromatography (HPLC) with diode array detection on an Agilent 1200 series chromatograph (Agilent Technologies, Inc, CA USA) at the Science and Technology Service Centre, Faculty of Science, Chiang Mai University (Chiang Mai, Thailand). This analysis followed the ISO/IEC 17025 method (International Organization for Standardization, 2005). The flow rate was 0.6 mL/min. The column used was a Zorbax Eclipse XDB-C18 (4.6 × 150 mm, 5 μm) and the absorption wavelength was selected at 280 nm. The mobile phase for detected chlorogenic acid and caffeic acid was a binary solvent system of 2 % acetic acid dissolved in HPLC water (solvent A) and absolute methanol (solvent B). Moreover, the mobile phase for detected protocatechuic acid, vanillic acid, and epicatechin was a binary solvent system of 0.1 % formic acid dissolved in HPLC water (solvent A) and absolute methanol (solvent B). In addition, total phenolic and anthocyanin contents were quantified using Folin-Ciocalteu reagent and vanillin assay, respectively, as previously described.[20,21]

2.3. Animals and induction of experimental type 2 diabetic rats

Forty-eight male Wistar rats weighing 170–220 g were obtained from Nomura Siam International, Bangkok, Thailand. The Laboratory Animal Care and Use Committee approved the animal facility and protocols at the University of Phayao, Phayao, Thailand (Protocol no. 640104013). All rats used in the experiment were housed in a controlled environment with a 12-h light and dark cycle. They were randomly divided into two groups: the normal diet group consumed a commercial normal chow diet (CP Mice Feed, no.082, Bangkok, Thailand) with 19.77 % of total energy from fat, while the high-fat diet group had access to food containing approximately 60 % of total energy from fat. After two weeks, the high-fat diet group received a single intraperitoneal injection of 40 mg/kg body weight of streptozotocin (STZ) dissolved in 0.09 M citrate buffer (Sigma-Aldrich; St. Louis, MO, USA). The normal diet group received a citrate buffer injection. A hundred microliter of blood samples were collected from the tail vein two weeks after the intraperitoneal injection of STZ, to determine overnight fasting blood glucose levels using a colorimetric assay (Erba Diagnostics, Mannheim, Germany). As shown in Fig. 1, rats with fasting blood glucose levels exceeding 250 mg/dL were considered diabetic.[22] Then, the rats were randomly divided into six groups (Table 1): normal diet (ND), ND supplemented with RRBE at 1000 mg/kg BW (ND + RRBE), type 2 diabetes (DM), DM supplemented with RRBE at 1000 mg/kg BW (DM + RRBE), DM treated with metformin at 70 mg/kg BW (DM + Met), and DM receiving a combination of RRBE at 1000 mg/kg BW and metformin at 70 mg/kg BW (DM + RRBE + Met). The selection of this single, high dose was due to our preliminary study demonstrating that after glucose loading, the plasma glucose level did not change over 120 min in 1000 mg/kg RRBE pretreated normal group. RRBE and metformin were dissolved in deionized water, and the rats received their respective supplements once daily for 12 weeks by oral gavage. Body weight was measured weekly, and food and water intake were recorded daily. Before sacrifice, an oral glucose tolerance test (OGTT) was conducted. The area under the curve (AUC) was calculated using GraphPad Prism version 10.0.3 (GraphPad Software, MA, USA). At the end of the experiment, the animals were euthanized using CO_2.

2.4. Biochemical analysis

Plasma glucose and triglyceride levels were measured using enzymatic colorimetric assay kits obtained from Erba Mannheim (ERBA Diagnostics Mannheim, FL, USA). The plasma insulin concentration was determined using Rat/Mouse Insulin ELISA assay kits (Merck KGaA, Germany). To assess insulin resistance, the homeostasis assessment of insulin resistance (HOMA) index was calculated using the formula: fasting plasma insulin (μU/mL) multiplied by fasting plasma glucose (mmol/L) divided by 22.5.[23]

2.5. Glucose transport in ex vivo rat jejunal loops

To address the effect of RRBE on glucose transport using an isolated jejunal loop, small intestinal tracts were removed, cleaned, and flushed with PBS. The jejunum was ligated to a length of 1.5 cm and intraluminally injected with PBS containing 2 mM 2-NBDG (Thermo Fisher Scientific, MA, USA) for 30 min. At the end of the experiment, the

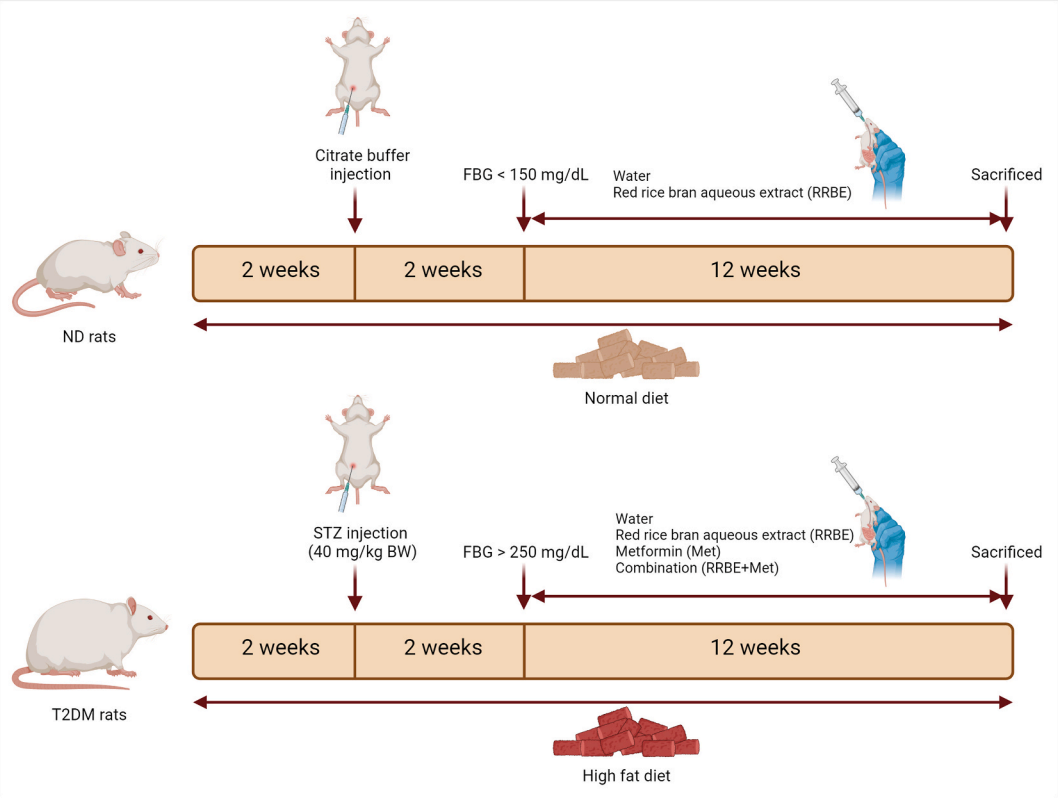

Fig. 1. Schematic representation of animals and induction of experimental model. Created with BioRender.com.

Table 1
Experimental groups and the number of animals.

Group abbreviation	Group description	Total number of animals included in the study
ND	Normal rats received a normal diet	6
ND + RRBE	ND supplemented with RRBE at 1000 mg/kg BW	6
DM	Type 2 diabetes mellitus rats	6
DM + RRBE	DM supplemented with RRBE at 1000 mg/kg BW	6
DM + Met	DM was treated with metformin at 70 mg/kg BW	6
DM + RRBE + Met	DM supplemented a combination of RRBE at 1000 mg/kg BW and metformin at 70 mg/kg BW	6

epithelial tissue was removed. The jejunal epithelium was dissolved in PBS. The fluorescence intensity was measured using a Synergy™ HT microplate reader (BioTek Instruments, Inc.) at excitation and emission wavelengths of 485 and 535 nm, respectively, and calculated as fmol/mg protein/min.

2.6. Histological analysis

The pancreas, a 1 cm segment of the jejunum, liver, and soleus muscle, were removed, fixed in 4 % paraformaldehyde at 4 °C for 12–24 h, rinsed with phosphate buffer saline (PBS), and then embedded in paraffin blocks. These paraffin blocks were later sliced into 5–7 μm thick sections and placed on slides coated with gelatin. The slides were stained using hematoxylin and eosin (H&E), following established protocols to assess the morphology of the pancreas and intestine and identify any abnormalities.[24] In addition, liver and soleus muscle slides were stained with periodic acid-Schiff base (PAS) for evaluated glycogen deposit in the tissues.

2.7. Hepatic and skeletal muscle glycogen content analysis

The hepatic and muscle glycogen levels determination were modified as previously described.[25] The frozen liver and soleus muscle were digested for 30 min in 30 % Potassium hydroxide (KOH) solution at 95 °C for glycogen determination. Its extraction was performed in two stages of precipitation by using 1 M of sodium sulfate (Na_2SO_4) and ethanol solution under heat and centrifuged at 20,000×*g* for 5 min. The pallets were washed twice with H_2O and ethanol. After that, the dried pellets were resuspended with 0.3 mg/mL amyloglucosidase and incubated at 37 °C for 3 h. The glucose levels were quantified by enzymatic colorimetric assay using commercial kits obtained from Erba Mannheim (ERBA Diagnostics Mannheim, FL, USA).

2.8. Immunofluorescence staining

Jejunum was excised, fixed in 4 % paraformaldehyde at 4 °C for 12–24 h, washed with PBS, and embedded in paraffin blocks. The sections were deparaffinized in xylene, rehydrated in gradient ethanol, and subjected to high-temperature antigen retrieval in citrate buffer (pH 6.0). Sections were blocked with 5 % BSA for 30 min and stained with rabbit anti-SGLT1 (Cat. No. 07-1402-I, Merck KGaA, Germany) and rabbit anti-GLUT2 (Cat. No. 07-1402-I, Merck KGaA, Germany), and Alexa Fluor 488-labeled rabbit (Thermo Fisher Scientific, MA, USA) was sequentially added. After immunoreaction, sections were incubated with DAPI (Thermo Fisher Scientific, MA, USA) for 5 min before mounting. Slides were detected using a Nikon Eclipse Ni–U fluorescent microscope (original magnification 40) (Nikon Corporation, Japan).

2.9. Subcellular fractionation and western blot analysis

Subcellular fractions were prepared through differential

centrifugation. The absorptive tissues of the jejunum were homogenized and centrifuged at 5000×*g* for 10 min at 4 °C, resulting in a supernatant referred to as the whole-cell lysate. Half of this supernatant underwent further centrifugation at 100,000 g for 2 h. The resulting supernatant represented the cytosolic fraction, while the pellet was resuspended in the same buffer and designated as the membrane fraction. The protein concentration in each sample was determined using a Bradford assay (Bio-Rad Laboratories, Inc.), and the samples were stored at −80 °C until further use. For Western blot analysis, the samples were mixed with 4X Laemmli solution, subjected to electrophoresis using 10 % SDS-PAGE, and transferred to PVDF membranes (Merck KGaA, Germany). Non-specific binding was blocked by incubating the membranes with 5 % (w/v) non-fat dry milk in 0.05 % Tween-20 in Tris-buffered saline (TBS-T) for 1 h at room temperature. The membranes were then incubated overnight at 4 °C with specific antibodies such as polyclonal anti-rabbit SGLT1 (1: 500, Cat. No. 07–1417, Merck), GLUT2 (1: 500, Cat. No. 07-1402-I, Merck KGaA, Germany), AMPK (Cat. No. AF3197, R&D Systems, MN, USA), p-AMPK (1: 500, Cat. No. 07–681, Merck KGaA, Germany), HNF-1α (1: 500, Cat. No. ab96777, Abcam, United Kingdom), monoclonal anti-mouse alkaline phosphatase (ALP) (1: 500, BBM marker; Cat. No. NB110-3638, Novus International, MO, USA), or anti-mouse β-actin (1: 500, Cat. No. ab8227, Abcam, United Kingdom) antibodies. Following washing with TBS-T buffer, the PVDF membranes were incubated with horseradish peroxidase-conjugated ImmunoPure secondary antibodies (goat anti-rabbit or anti-mouse IgG) for 1 h at room temperature. Protein bands were visualized using Clarity Western ECL Substrate (Bio-Rad Laboratories, Inc.) and semi-quantitatively analyzed using ImageJ version 1.44p (National Institutes of Health).

2.10. Statistical analysis

Data were expressed as mean ± SEM. Statistical differences were assessed using one-way ANOVA followed by Tukey's post hoc test. Statistical analyses were conducted using Statistical Package for IBM SPSS Statistical Software version 23 (IBM Corp., NY, USA). Differences were considered to be significant when $p < 0.05$.

3. Results

3.1. Phenolic compounds in RRBE

HPLC chromatogram of RRBE reliably detected protocatechuic acid, caffeic acid, vanillic acid, and epicatechin with retention time at 7.239, 8.486, 22.264, and 27.626 min (Fig. 2B and D). The calculated amount of each significant constituent found in RRBE, as obtained from their respective calibration curves, is shown in Table 2. Compared to other phenolic compounds, a high epicatechin content was obtained (15.5 mg/kg). In addition, protocatechuic acid was found at 11.2 mg/kg of RRBE, whereas vanillic acid and caffeic acid were present at 5.32 and 0.55 mg/kg of RRBE, respectively (Table 2). As shown in Table 3, the total phenolic content of RRBE was 871.22 ± 12.24 mg gallic acid equivalents (GAE)/kg RRBE. The anthocyanin content was 6.20 ± 0.24 mg catechin/g RRBE.

3.2. Effects of RRBE on general characteristics, glucose tolerance, and pancreatic morphology in T2DM rats

As indicated in Table 4, There was no significant difference in body weight among the experimental groups. T2DM rats demonstrated significantly higher plasma glucose and triglyceride levels than the ND group. Once again, these values were significantly reduced in DM + RRBE, DM + Met, and DM + RRBE + Met rats compared to the T2DM group. Although no significant differences were observed in plasma insulin levels among the experimental groups, the HOMA index, which indicates insulin resistance, was significantly elevated in T2DM rats. However, RRBE, metformin, and the combination treatment showed a decrease in this parameter. This suggests that RRBE provided benefits in improving hyperglycemia, hypertriglyceridemia, and insulin resistance in T2DM rats as well as metformin. Similar to the typical characteristics of T2DM, the results demonstrated that T2DM rats exhibited glucose intolerance, as indicated by a significant increase in AUC (1613.83 ± 46.68 mg x min/dL, $p < 0.05$). However, T2DM rats treated with RRBE 952.67 ± 111.00 mg x min/dL, $p < 0.05$), metformin (881.58 ± 126.70 mg x min/dL, $p < 0.05$), or combination treatment (801.32 ± 45.38 mg x min/dL, $p < 0.05$) showed a significantly reduced AUC compared to

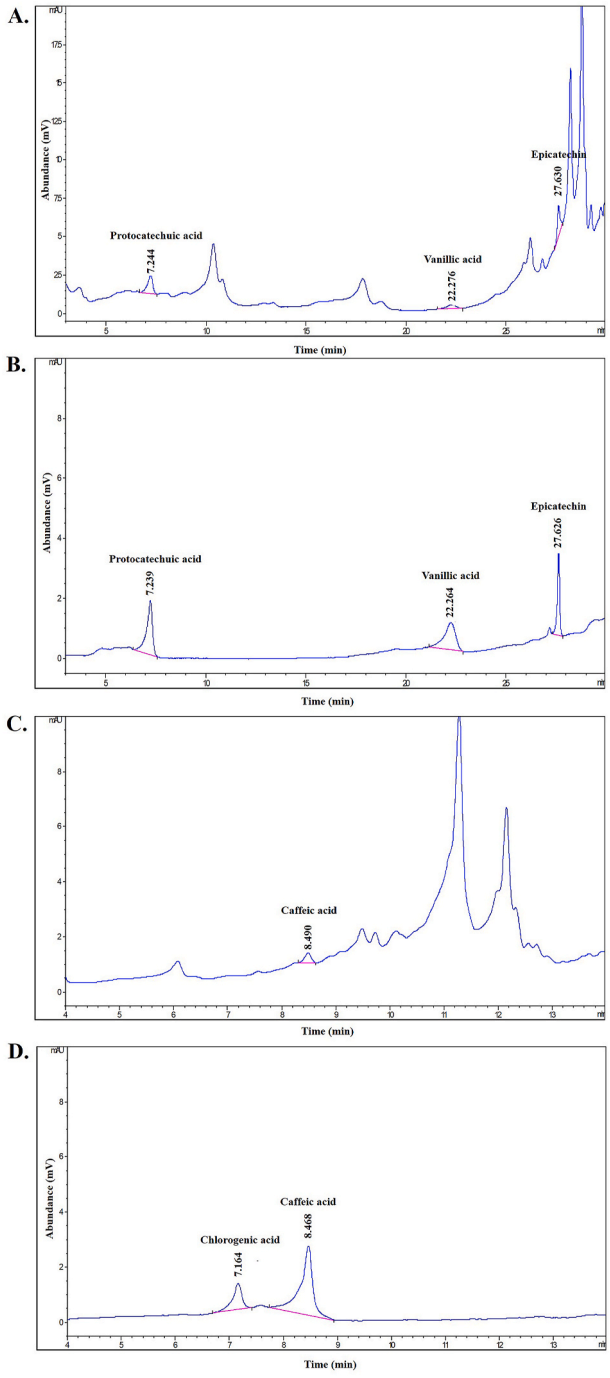

Fig. 2. A representative HPLC chromatogram of (A) Red rice bran aqueous extract (RRBE) for detect chlorogenic acid and caffeic acid contents, (B) chlorogenic acid and caffeic acid standard, and (C) red rice bran aqueous extract (RRBE) for detect protocatechuic acid, vanillic acid, and epicatechin (D) protocatechuic acid, vanillic acid, and epicatechin standards at the absorption wavelength 280 nm.

Table 2
The quantification parameters and quantitative amount of significant components in red rice bran aqueous extract (RRBE).

Major component	Amount (mg/kg of RRBE)
Epicatechin	15.5
Protocatechuic acid	11.2
Vanillic acid	5.32
Caffeic acid	0.55
Chlorogenic acid	ND

Table 3
Total phenolic contents and anthocyanin of RRBE.

Bioactive	Amount
Total phenolic content (mg GAE/kg RRBE)	871.22 ± 12.24
Anthocyanin (mg Catechin/g RRBE)	6.20 ± 0.24

T2DM rats (Fig. 3A and B). These findings suggest that RRBE has anti-diabetic effects against hyperglycemia, hyperlipidemia, insulin resistance, and glucose intolerance.

To further investigate the pancreatic protective effects of RRBE, a morphological analysis was performed using standard methods for tissue biopsy, i.e., hematoxylin and eosin (H&E) staining. Fig. 3C and D shows that ND and ND + RRBE demonstrated normal pancreatic islet structures. Moreover, a microscopic examination of pancreatic tissues of the diabetic group showed the pancreatic islets of Langerhans were damaged, as indicated by disrupted islet integrity and uneven boundaries (blue arrow), vacuolation (green arrow) and decreased vasculature with cellular infiltration with cells as lymphocytes and mononuclear cells with focal areas of degeneration, congestion, and necrosis (red arrow) (Fig. 3E) compared to normal patterns. Furthermore, the pancreatic morphology in DM + Met still showed islet integrity disruption and uneven boundaries (blue arrow) (Fig. 3G). Treatment with the RRBE and combination with metformin and RRBE resulted in pancreatic morphologies resembling those of normal rats (Fig. 3F and H).

3.3. RRBE inhibited glucose uptake in intestinal absorptive tissues

The inhibitory effect of RRBE on glucose absorption was evaluated. As shown in Fig. 4A, the intestinal fluorescent glucose analog uptake level was significantly higher in T2DM rats (592.63 ± 71.98 fmol/mg protein, $p < 0.05$) when compared with ND rats. In addition, this level was significantly reduced in DM + RRBE (367.72 ± 62.42 fmol/mg protein, $p < 0.05$), DM + Met (274.00 ± 32.08 fmol/mg protein, $p < 0.05$), and DM + RRBE + Met rats (167.67 ± 12.45 fmol/mg protein, $p < 0.05$) compared to the T2DM group, suggesting that RRBE ameliorated intestinal glucose absorption in T2DM.

To further investigate the effect of RRBE on jejunal epithelial tissue morphology, hematoxylin, and eosin (H&E) staining was performed. As shown in Fig. 4B–G, there were no differences in the jejunal tissue structures among experimental groups, suggesting that the diabetes condition in this study did not affect jejunal absorptive tissues. Thus, this study clearly shows that a high-fat diet combined with a low dose of STZ not altered intestinal morphology but increased intestinal glucose transport function.

3.4. RRBE interfered with intestinal glucose uptake via downregulated sodium/glucose cotransporter protein 1 (SGLT1)

To evaluate whether the inhibited intestinal glucose transport caused by RRBE was due to the downregulation of SGLT apical membrane expression, intestinal SGLT1 protein expression was determined using immunofluorescence. The results show that the immunostaining for apical membrane SGLT1 showed no difference between ND (Fig. 5A) and ND + RRBE (Fig. 5B) rats. Moreover, the SGLT1 glucose transporter was increased in brush border membrane (BBM) SGLT1 expression (white arrow) in Type 2 DM rats (Fig. 5C). In T2DM rats receiving RRBE (Fig. 5D), MET (Fig. 5E), and RRBE + Met (Fig. 5F) rats, the expression of SGLT1 protein was downregulated in the intestinal epithelium.

This study further confirmed the effects of RRBE on SGLT1 expression using Western blot. As shown in Fig. 5G, intestinal membrane SGLT1 protein expression was significantly decreased in DM + RRBE treated group (0.32 ± 0.11 a. u., $p < 0.05$), while metformin and RRBE combined with metformin were not different compared to that of T2DM rats. However, there were no significant differences in cytosolic fraction among groups (Fig. 5H). The data presentation suggests that RRBE-induced down-regulation of SGLT1 membrane protein expression reduced glucose uptake in the T2DM rat model.

3.5. RRBE suppressed glucose transporter 2 (GLUT2) expression leading to decreased intestinal glucose transport

After RRBE treatment, the expression of GLUT2 was not different between ND and ND + RRBE-treated rats (Fig. 6A and B). However, the elevation of GLUT2 expression at the intestinal apical membrane was observed in T2DM rats, as shown with green fluorescence (Fig. 6C). Surprisingly, this elevation was reduced in RRBE, metformin, and combination-treated groups (Fig. 6D, E, and F). The subcellular distribution changes of GLUT2 in intestinal epithelial cells were further studied. The results showed that GLUT2 was increased in localization in the membrane fraction of intestinal epithelial cells in diabetic rats (1.17 ± 0.26 a. u., $p < 0.05$) (Fig. 6G). Moreover, treated with RRBE (0.22 ± 0.0.09 a. u., $p < 0.05$), metformin (0.45 ± 0.17 a. u., $p < 0.05$), and RRBE + Met (0.41 ± 0.02 a. u., $p < 0.05$) for 12 weeks decreased intestinal epithelium membrane GLUT2 expression, as shown in Fig. 6G. Although GLUT2 protein expression was reduced in the cytosol fraction of the DM group (0.15 ± 0.07 a. u., $p < 0.05$), it was not significantly reduced in all treatment groups (Fig. 6H).

3.6. RRBE did not downregulate glucose transporters via phosphorylation of AMPK or HNF1α

As shown in Fig. 7A, the activation of AMPK was elevated in the DM + Met (1.08 ± 0.09 a. u., $p < 0.05$) and DM + RRBE + Met groups (1.30 ± 0.09 a. u., $p < 0.05$). These results implied that the activation of AMPK in DM + RRBE + Met rats might be due to metformin drugs. Fig. 7B showed the expression of HNF1α was no different between ND and ND + RRBE groups. Moreover, HNF1α increased in T2DM intestinal epithelium tissue (2.39 ± 0.22 a. u., $p < 0.05$). However, it was not significantly decreased in all treatment groups. Therefore, these data suggest that RRBE might be inhibited by GLUT2 transport function and expression via other regulators.

Table 4
The effect of RRBE on general characteristics and plasma parameters in type 2 diabetes mellitus (T2DM) rats.

	ND	ND + RRBE	DM	DM + RRBE	DM + Met	DM + RRBE + Met
Body weight (g)	490.00 ± 16.16	478.58 ± 25.45	549.29 ± 25.92	524.17 ± 21.58	502.86 ± 13.40	479.17 ± 36.22
Glucose (mg/dL)	96.19 ± 15.62	127.74 ± 24.53$^{\#}$	272.98 ± 22.32*	142.08 ± 29.29$^{\#}$	142.26 ± 17.41$^{\#}$	146.17 ± 34.56$^{\#}$
Insulin (ng/mL)	6.43 ± 1.12	6.20 ± 0.72	5.87 ± 1.05	5.51 ± 0.57	5.33 ± 0.95	6.08 ± 1.27
HOMA index	34.23 ± 5.35	40.90 ± 4.45$^{\#}$	63.54 ± 3.54*	40.90 ± 7.69$^{\#}$	36.41 ± 4.52$^{\#}$	41.92 ± 5.23$^{\#}$
Triglycerides (mg/dL)	80.20 ± 8.86	76.73 ± 12.61$^{\#}$	331.51 ± 35.69*	176.79 ± 32.14$^{\#}$	193.16 ± 15.64$^{\#}$	162.43 ± 22.65$^{\#}$

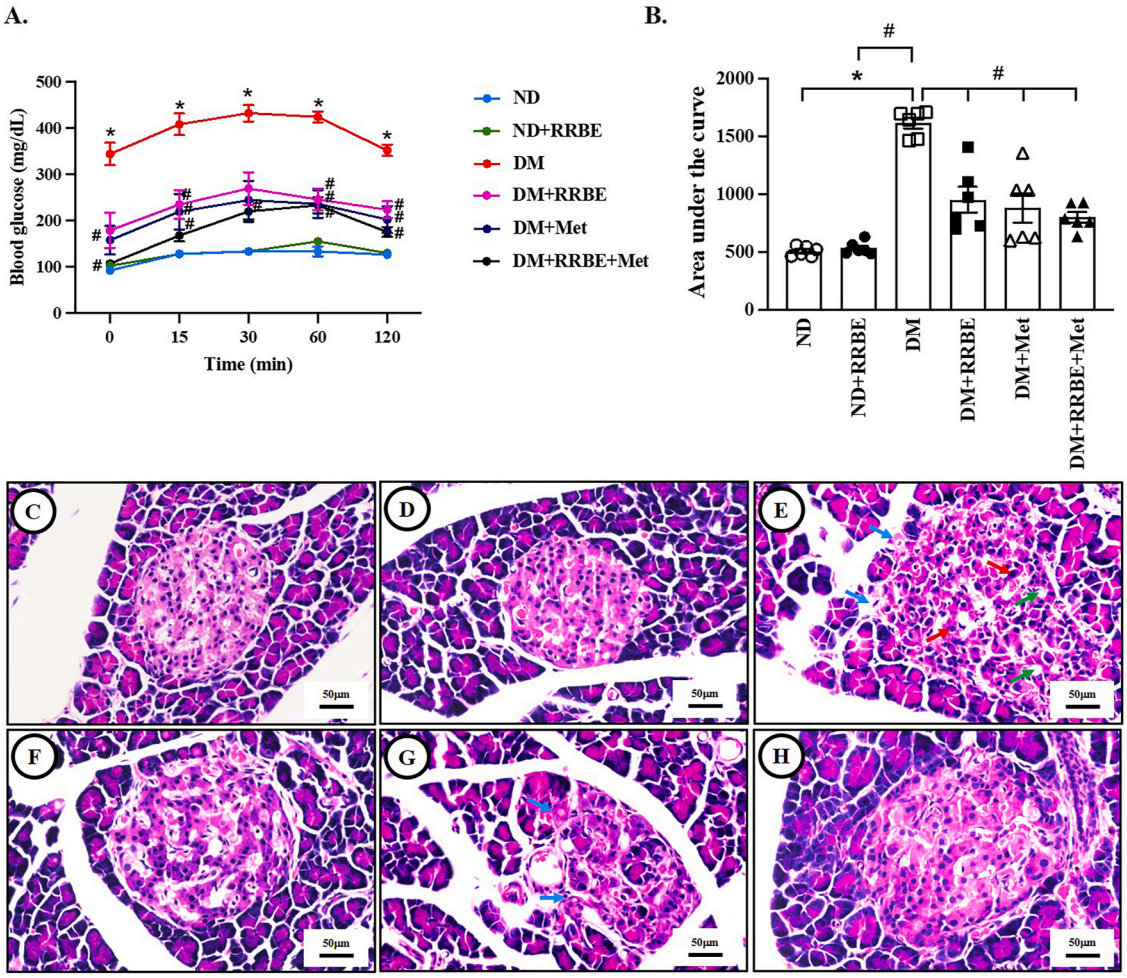

Fig. 3. The impact of RRBE on glucose intolerance in type 2 diabetic (T2DM) rats. Blood glucose levels were measured at the baseline and after glucose loading (1 g/kg BW) for 120 min. (A) Plasma glucose levels were determined using a commercially available colorimetric assay. (B) The total area under the curve (AUC) was calculated based on the data from (A). The results are presented as mean ± SEM (n = 6), *p < 0.05 compared to the ND group, #p < 0.05 to the T2DM group. (C–H) Microscopic images of pancreas tissues stained with conventional hematoxylin and eosin (H&E). (C) Normal diet (ND), (D) ND treated with RRBE (ND + RRBE), (E) T2DM rat (DM), (F) T2DM treated with RRBE (DM + RRBE), (G) T2DM treated with metformin (DM + Met), (H) T2DM treated with RRBE and metformin (DM + RRBE + Met). Pancreas samples from each experimental group were collected, fixed, embedded, sectioned, and stained with H&E (original magnification 40x). The assay was repeated at least three times using different sets of animals. The data were subsequently analyzed using bright-field microscopy.

3.7. Combination with RRBE and metformin decrease blood glucose by elevating glycogen accumulation in soleus muscle and liver tissues

To further investigate the effect of RRBE on glycogen content, tissue glycogen extraction and Periodic acid–Schiff (PAS) staining were performed. The liver glycogen contents were significantly decreased in the DM group (129.09 ± 6.37 mg/g protein, $p < 0.05$) compared to the ND group (278.61 ± 29.70 mg/g protein, $p < 0.05$) (Fig. 8A). Furthermore, this content was significantly elevated in the DM + RRBE + Met group (273.09 ± 47.63 mg/g protein, $p < 0.05$) compared to the DM group. The results of the PAS staining of the liver cross-section are confirmed in Fig. 8B–G. The glycogen accumulation showed a greater positively stained area (purple color) in ND (Fig. 8B) and ND + RRBE (Fig. 8C) than in the diabetic rats (Fig. 8D). Treatment with the combination of RRBE and metformin appeared to elevate the level of positive staining (Fig. 8G).

Similarly, glycogen accumulation in the soleus muscle was markedly reduced in the DM rats (12.49 ± 1.38 mg/g protein, $p < 0.05$) compared to the control (31.63 ± 3.52 mg/g protein, $p < 0.05$) (Fig. 8H). Furthermore, the glycogen content was significantly increased in the DM + RRBE + Met group (27.61 ± 2.57 mg/g protein, $p < 0.05$). Again, the PAS staining of the soleus muscle in each group is confirmed in Fig. 8I-N. The ND (Fig. 8I) and ND + RRBE (Fig. 8J) have a greater positive stained area than the DM group (Fig. 8K). However, supplementing with RRBE + Met increased the positive staining area (Fig. 8N). These data suggest combining red rice bran aqueous extract and metformin can improve glycogen storage in DM rats' liver and soleus muscle.

4. Discussion

This study was to investigate the beneficial effects of RRBE in diabetic conditions. RRBE at 1000 mg/kgBW of RRBE in this study can be converted to a human dose at 9720 mg/60kgBW/day, according to a previous study.[26] As shown in Table 4, fasting plasma glucose, HOMA index, and triglyceride levels were markedly increased in our experimental model. These levels were reduced in RRBE, metformin, and a combination of RRBE and metformin-treated rats. A previous study reported that epicatechin, the highest component in RRBE, mitigated insulin signaling impairment and diabetes conditions in high fructose-fed rats.[27] Moreover, high fat-fed mice supplemented with epicatechin at 200 mg/kg diet reduced body weight gain and improved insulin sensitivity.[28] Accordingly, protocatechuic acid also showed a stimulation effect on insulin signaling in the human adipocytes of obese subjects,[29]

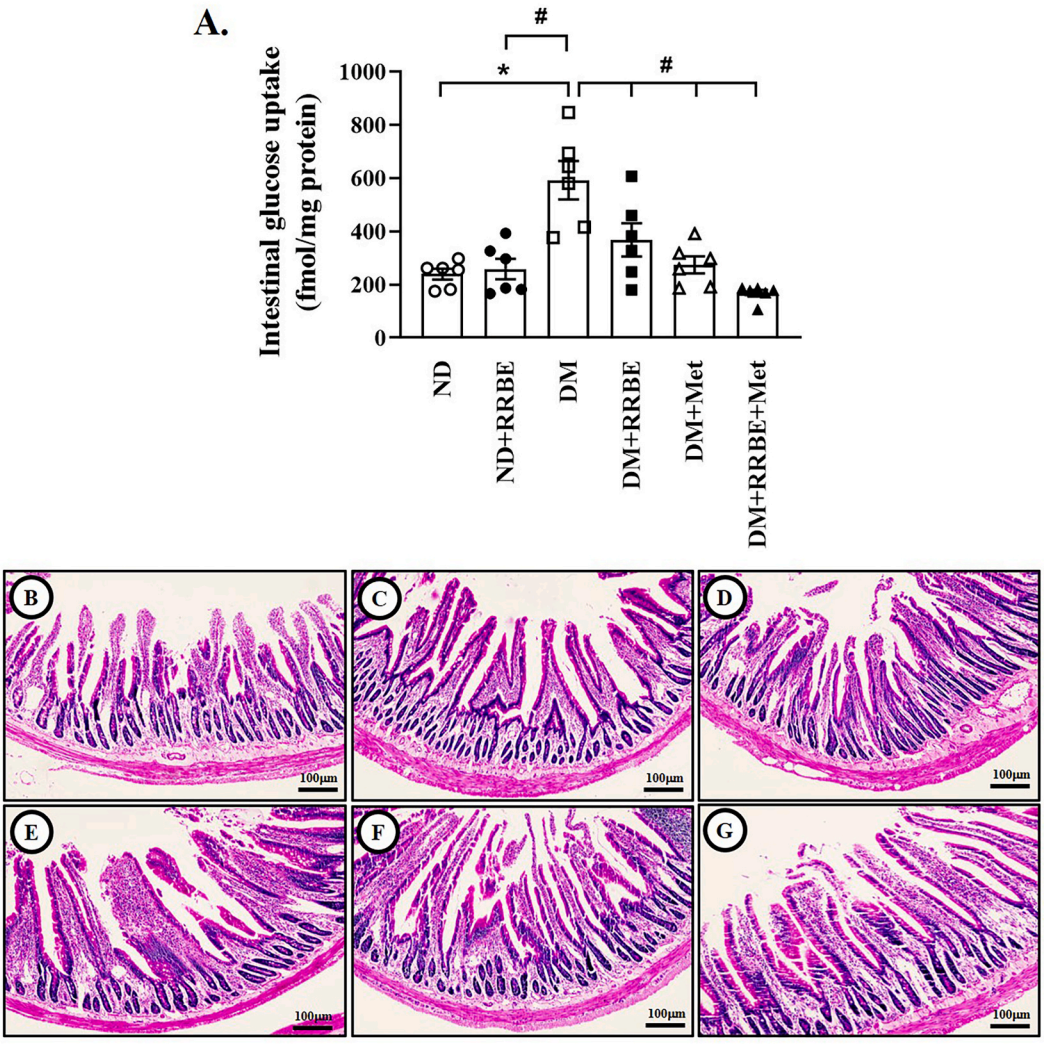

Fig. 4. Effect of RRBE on glucose transport using *ex vivo* rat jejunal loops. (A) 2 mM 2-NBDG was injected in a rat jejunal loop and incubated for 30 min. The fluorescent intensity in the intestinal epithelium was then measured and expressed as intensity/mg protein. Values are mean ± SEM (n = 6), *p < 0.05, vs. control, #p < 0.05 vs. the T2DM group. (B–G) Micrographs of conventional hematoxylin and eosin (H&E) staining of the jejunal epithelial tissues. (B) Normal diet (ND), (C) Normal diet treated with RRBE (ND + RRBE), (D) T2DM rat (DM), (E) T2DM treated with RRBE (DM + RRBE), (F) T2DM treated with metformin (DM + Met), (G) T2DM treated with RRBE and metformin (DM + RRBE + Met). The jejunum from each experimental group was removed, fixed, embedded, cut, and stained by H&E (original magnification 10x). The assay was performed at least three times on separate sets of animals. The data were then analyzed using bright-field microscopy.

implying it might potentially be involved in RRBE's anti-diabetic action.

The present study shows that RRBE decreased diabetic status by reducing jejunal glucose absorption in high fat/streptozotocin-induced diabetic rats. Previous evidence suggests that increment of intestinal glucose absorption plays a major role in postprandial hyperglycemia resulting in T2DM.[30,31] As mentioned earlier, the transepithelial transport of glucose in the small intestine can be mediated by an active absorption through SGLT1 and by a diffusive component GLUT2 at the BBM.[32] We found that glucose absorption was increased in diabetic rats, mainly shown by the localization of SGLT1 and GLUT2 in the brush border membrane of jejunal epithelium in high-fat/streptozotocin-induced diabetic rats. There is an increasing accumulation of data linking natural compounds with effects on glucose transporters inhibition and intestinal glucose absorption. Thus, there is the potential for these compounds to protect against the development of type 2 diabetes and metabolic syndrome. Of particular relevance to the present study are observations that RRBE suppressed SGLT1 and GLUT2 expression at the BBM of enterocytes, decreasing intestinal glucose uptake. There are several natural compounds have been reported to inhibit these transporters. For example, flavonoids from the roots of *Sophora flavescens* inhibit methyl-α-*d*-glucopyranoside uptake through SGLT1 in monkey kidney fibroblast-like cells.[33] Mulberry leaf polyphenols suppress glucose transport via SGLT1 in the human colon carcinoma cell line (Caco-2).[34] Furthermore, epicatechin gallate is a potent inhibitor of glucose uptake into intestinal cells and a competitive inhibitor of the SGLT1, expressed on the apical membrane of small intestinal enterocytes.[35,36]

One significant SGLT1 and GLUT2 regulator is the metabolic sensing kinase AMP-dependent kinase (AMPK). It has been reported that the activation of AMPK with AICAR in mice jejunal tissue results in an increase in glucose uptake that can be attributed to an increased amount of GLUT2 in the BBM.[37] Furthermore, epidermal growth factor upregulated SGLT1 and GLUT2 via EGFR/AMPK signaling pathway to jointly promote intestinal glucose absorption in lipopolysaccharide-induced IPEC-J2 cells and piglets.[38] In contrast, our previous study reported that caffeic acid rich in coffee bean extract inhibited SGLT1 and GLUT2-mediated AMPK phosphorylation in Caco-2 cells.[39] This study reported that RRBE reduced intestinal SGLT1 and GLUT2 membrane expression without changing the p-AMPK levels. Additionally, the phosphorylation of AMPK was found in the DM + Met and DM + RRBE

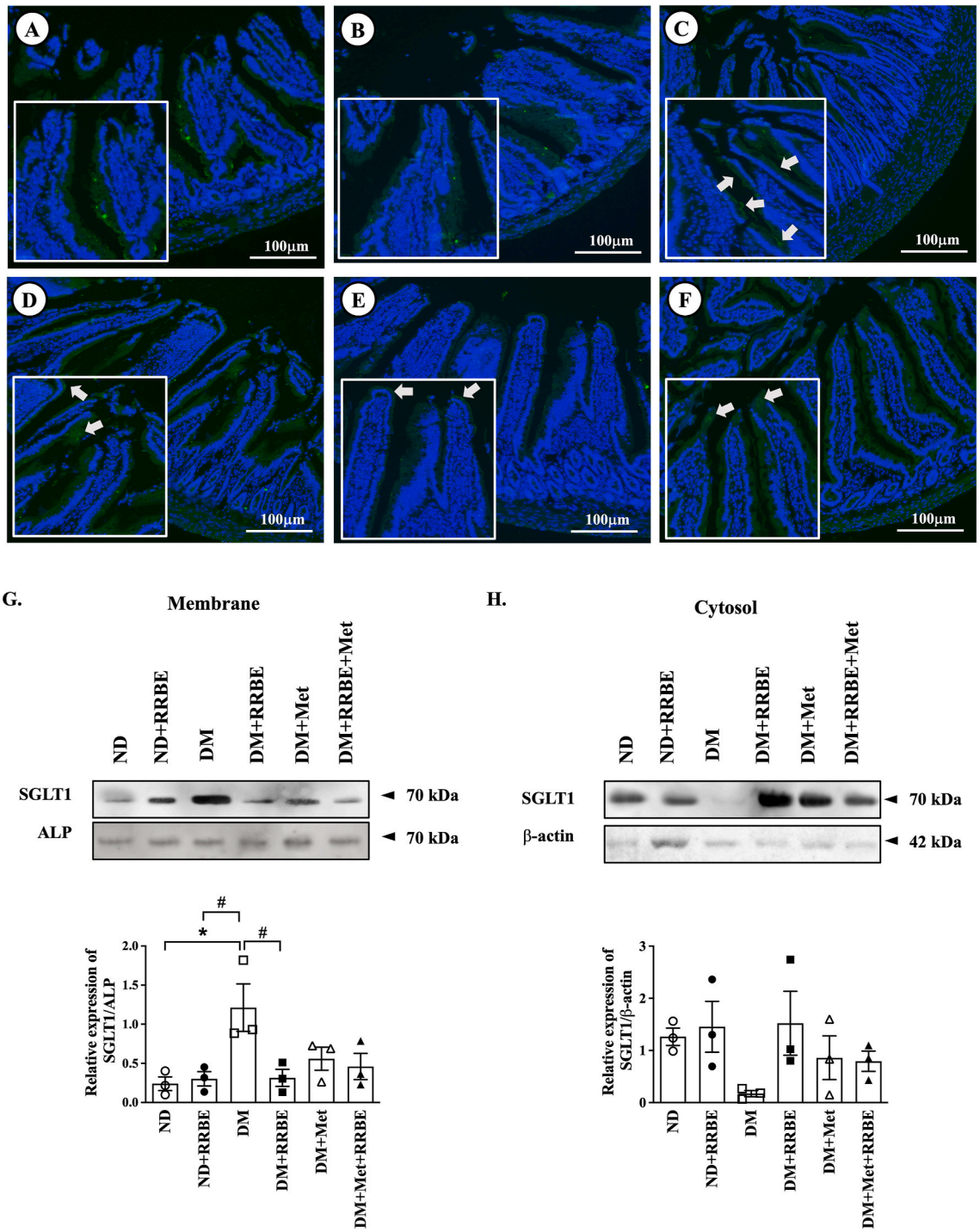

Fig. 5. Effect of RRBE on sodium/glucose cotransporter protein 1 (SGLT1) expression in jejunal epithelial tissues. (A) Normal diet (ND), (B) Normal diet treated with RRBE (ND + RRBE), (C) T2DM rat (DM), (D) T2DM treated with RRBE (DM + RRBE), (E) T2DM treated with metformin (DM + Met), (F) T2DM treated with RRBE and metformin (DM + RRBE + Met). SGLT1 transporter expressions were shown in green color (white arrow). Nuclei were stained with DAPI (blue). The original magnification is 10x. (G) Representative blot of SGLT1 membrane protein expression and semi-quantification of relative SGLT1/ALP protein expression, (H) representative blot of SGLT1 cytosol protein expression and semi-quantification of relative SGLT1/β-actin protein expression. Values are presented as the mean ± the standard error of the mean (n = 3). *p < 0.05 vs. the ND group, #p < 0.05 vs. the T2DM group.

+ Met groups; however, GLUT2 expression was decreased in DM + RRBE, DM + Met, and DM + RRBE + Met rats, while SGLT1 expression only decreased in DM + RRBE rats. HNF1α is a transcription factor SGLT1 expression in cultured enterocytes.[40] Moreover, the expression pattern of GLUT2 in several organs, including pancreatic β-cells, hepatocytes, intestine, and kidney, is similar to that of HNF-1α. Thus, HNF-1α might be vital in regulating GLUT2 expression and function.[41,42] Nevertheless, this study found that HNF1α expression was not different among the diabetic-treated group. Therefore, the effect of the RRBE on the expression and function of glucose transporter proteins might be caused by other regulators.

Glycogen is the storage form of glucose in the liver and muscles. Liver glycogen regulates blood glucose homeostasis, while muscle glycogen fuels muscles during intense exertion. The breakdown of liver

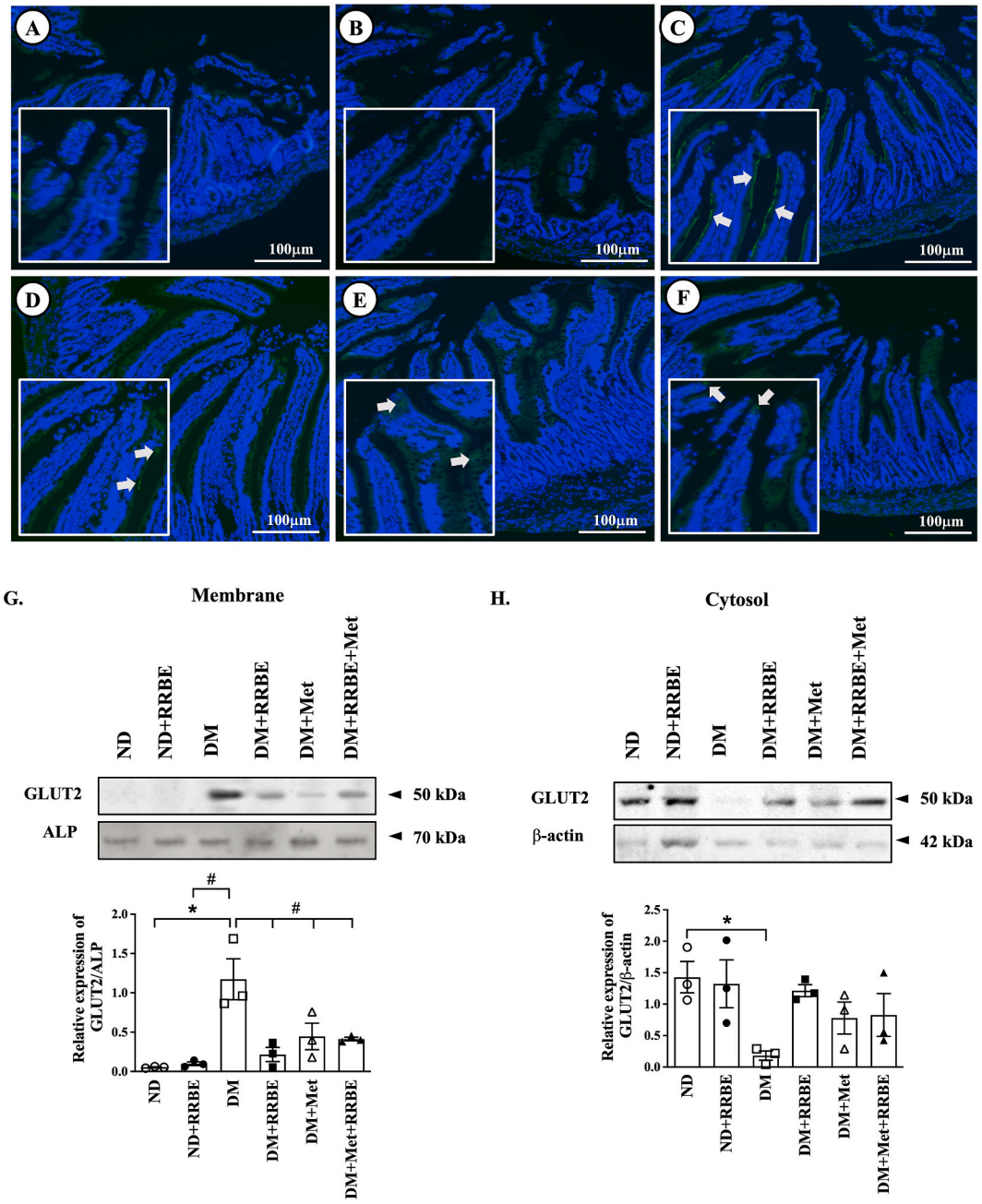

Fig. 6. Effect of RRBE on Glucose Transporter 2 (GLUT2) expression in jejunal epithelial tissues. (A) Normal diet (ND), (B) Normal diet treated with RRBE (ND + RRBE), (C) T2DM rat (DM), (D) T2DM treated with RRBE (DM + RRBE), (E) T2DM treated with metformin (DM + Met), (F) T2DM treated with RRBE and metformin (DM + RRBE + Met). GLUT2 transporter expressions were shown in green color (white arrow). Nuclei were stained with DAPI (blue). The original magnification is 10x. (G) Representative blot of GLUT2 membrane protein expression and semi-quantification of relative GLUT2/ALP protein expression, (H) representative blot of GLUT2 cytosol protein expression, and semi-quantification of relative GLUT2/β-actin protein expression. Values are presented as the mean ± the standard error of the mean (n = 3). *p < 0.05 vs. the ND group, #p < 0.05 vs. the T2DM group.

glycogen helps regulate blood glucose levels, while muscle glycogen supports energy needs during strenuous activities.[43] T2DM reduces liver and muscle glycogen content due to decreasing insulin signaling.[44] Conversely, glycogen accumulates in the heart and pancreatic β-cells in T2DM.[45] Moreover, glycogen accumulates in adipose tissue in obese insulin-resistant patients.[46] The rate-limiting enzymes in the gluconeogenic process are glucose-6-phosphatase (G6Pase) and phosphoenolpyruvate carboxyl kinase (PEPCK),[47] which is the diabetic treating target.[48] (−)-Epicatechin-3-*O*-β-*d*-allopyranoside rich in *Davallia formosana* decreased PEPCK and G6Pase mRNA expression, leading to increased glycogen accumulation and reduced glucose production.[49] Moreover, RRBE's major component, protocatechuic acid, also attenuated PEPCK and G6Pase mRNA expression.[50] Similarly, this study also showed liver and muscle glycogen levels decreased in the DM group; however, glycogen accumulation was elevated in DM treated with RRBE and metformin. Thus, the enhancement of liver and skeletal muscular glycogen synthesis in RRBE + Met-treated rats might be due to the inhibitory effect of RRBE on these enzymes. Finally, it can be indicated that not only inhibited intestinal glucose transporters by RRBE but also increased liver and muscle glycogen accumulation that can attenuate diabetic condition in this study. However, it should be noted that the anti-diabetic effect of RRBE and its mechanisms require further

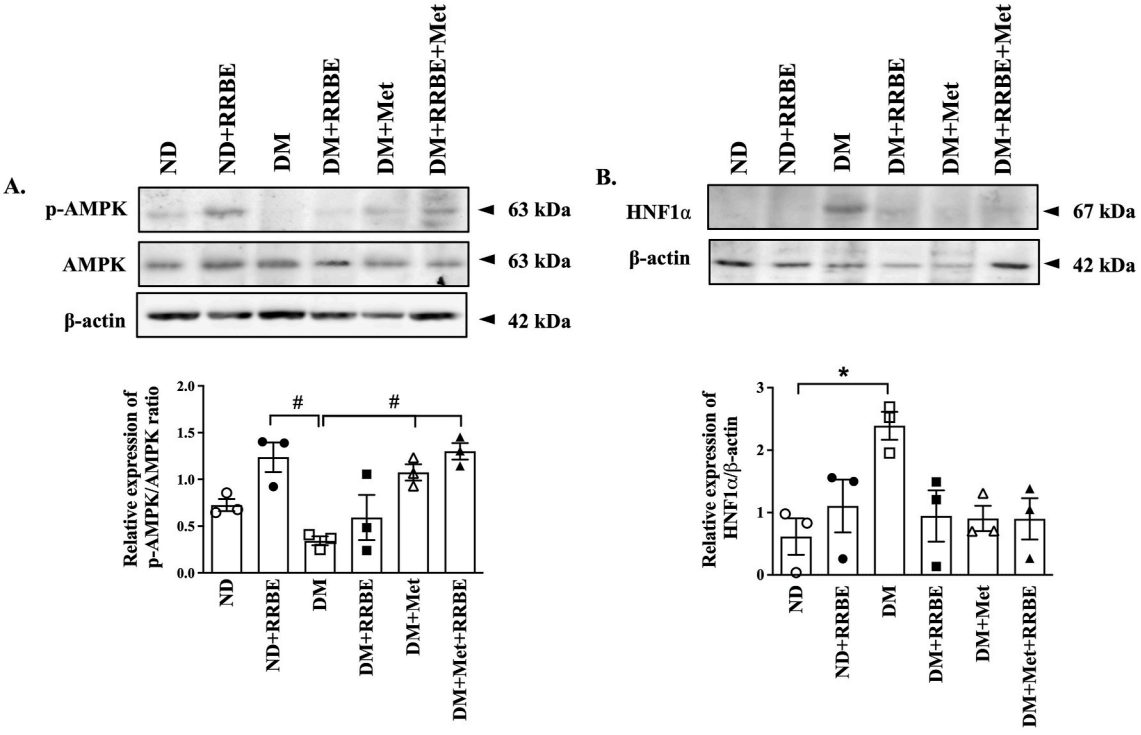

Fig. 7. Effect of RRBE on AMP-activated protein kinase (AMPK) and Hepatocyte nuclear factor 1 alpha (HNF1α) expression in jejunal epithelial tissues. (A) Representative blot of total and phosphorylation form of AMPK protein expression and semi-quantification of relative AMPK/β-actin protein expression and (B) Representative blot of total and phosphorylation form of HNF1α protein expression and semi-quantification of relative HNF1α/β-actin protein expression. Values are presented as the mean ± the standard error of the mean (n = 3). *p < 0.05 vs. the ND group, #p < 0.05 vs. the T2DM group.

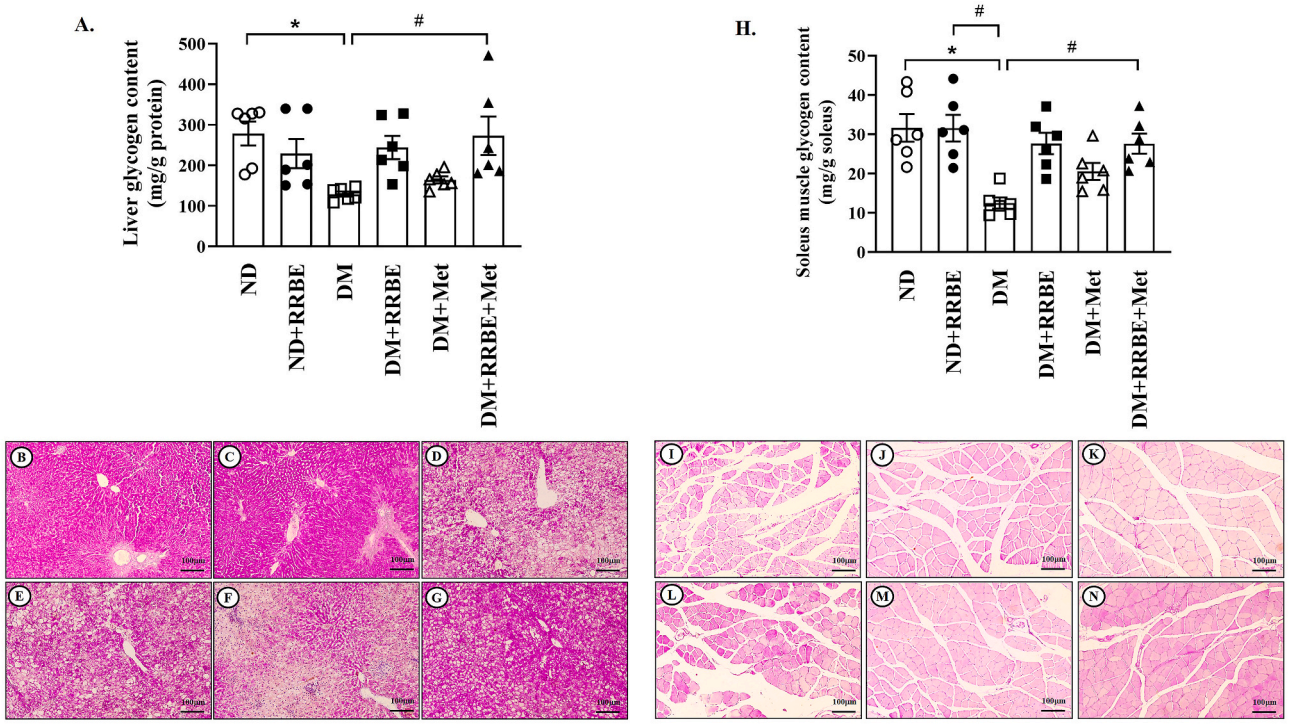

Fig. 8. Effect of RRBE on glycogen accumulation in the liver and soleus muscle. (A) Glycogen content in the livers. Values are presented as the mean ± the standard error of the mean (n = 6). *p < 0.05 vs. the ND group, #p < 0.05 vs. the T2DM group. The periodic acid-Schiff (PAS) staining of liver sections (B) Normal diet (ND), (C) Normal diet treated with RRBE (ND + RRBE), (D) T2DM rat (DM), (E) T2DM treated with RRBE (DM + RRBE), (F) T2DM treated with metformin (DM + Met), (G) T2DM treated with RRBE and metformin (DM + RRBE + Met). (H) Glycogen content in the soleus muscle. Values are presented as the mean ± the standard error of the mean (n = 6). *p < 0.05 vs. the ND group, #p < 0.05 vs. the T2DM group. The PAS staining of soleus muscle sections (I) Normal diet (ND), (J) Normal diet treated with RRBE (ND + RRBE), (K) T2DM rat (DM), (L) T2DM treated with RRBE (DM + RRBE), (M) T2DM treated with metformin (DM + Met), (N) T2DM treated with RRBE and metformin (DM + RRBE + Met). The original magnification is 10x.

investigation in clinical trials.

In conclusion, RRBE downregulated intestinal glucose transporters' expression, reducing glucose uptake. Consequently, RRBE attenuated hyperglycemia, hyperlipidemia, insulin resistance, and glycogen accumulation. This magnificent effect of RRBE makes it a new alternative approach as a natural anti-diabetic-supplement. However, it should be noted that the antidiabetic effect of RRBE and its mechanisms requires further investigation in clinical trials.

Funding statement

This research was supported by the National Higher Education Science Research and Innovation Policy Council (Grant no. FF64-RIB008 to AO).

Authors' contributions

Atcharaporn Ontawong: Conceptualization, Methodology, Investigation, Data curation, Writing – original draft, Project administration, Funding acquisition. **Sirinat Pengnet**: Methodology, Investigation, Data curation, Resources. **Arthid Thim-Uam**: Investigation, Validation, Resources. **Chutima S. Vaddhanaphuti**: Methodology, Validation, Writing – review & editing. **Narongsuk Munkong**: Investigation, Data curation. **Manussaborn Phatsara**: Investigation, Validation. **Kullanut Kuntakhut**: Investigation. **Jakkapong Inchai**: Investigation. **Doungporn Amornlerdpison**: Validation, Resources. **Teerawat Rattanaphot**: Investigation.

Declaration of interest statement

None.

Acknowledgments

The authors thank Mr. Prathakphong Riyamongkol and Mr. Dej Mann for their animal handling and feeding assistance; and Ms. Lamaiporn Peerapapong for technical assistance.

Abbreviation

ALP	alkaline phosphatase
AMPK	5′ AMP-activated protein kinase
BW	body weight
BBM	brush border membrane
GAE	gallic acid equivalents
GLUT2	glucose transporter 2
H&E	hematoxylin and eosin
HNF1α	hepatocyte nuclear factor 1 alpha
HPLC	high-performance liquid chromatography
HOMA	homeostasis assessment of insulin resistance
2-NBDG	2-(N-(7-nitrobenz-2-oxa-1,3-diazol-4-yl)amino)-2-deoxyglucose
p-AMPK	phosphorylation of AMPK
KOH	potassium hydroxide
RRBE	red rice bran aqueous extract
SGLT1	sodium-dependent glucose cotransporter 1
Na_2SO_4	sodium sulfate
STZ	streptozotocin
TBS-T	tris-buffered saline
T2DM	type 2 diabetes

References

1. Koepsell H. Glucose transporters in the small intestine in health and disease. *Pflügers Archiv*. 2020;472(9):1207–1248. https://doi.org/10.1007/s00424-020-02439-5.
2. Sun B, Chen H, Xue J, Li P, Fu X. The role of GLUT2 in glucose metabolism in multiple organs and tissues. *Mol Biol Rep*. 2023;50(8):6963–6974. https://doi.org/10.1007/s11033-023-08535-w.
3. Sano R, Shinozaki Y, Ohta T. Sodium-glucose cotransporters: functional properties and pharmaceutical potential. *J Diabetes Investig*. 2020;11(4):770–782. https://doi.org/10.1111/jdi.13255.
4. Ferraris RP, Yasharpour S, Lloyd KC, Mirzayan R, Diamond JM. Luminal glucose concentrations in the gut under normal conditions. *Am J Physiol*. 1990;259(5 Pt 1):G822–G837. https://doi.org/10.1152/ajpgi.1990.259.5.G822.
5. Miyamoto K, Hase K, Taketani Y, et al. Diabetes and glucose transporter gene expression in rat small intestine. *Biochem Biophys Res Commun*. 1991;181(3):1110–1117. https://doi.org/10.1016/0006-291x(91)92053-m.
6. Fujita Y, Kojima H, Hidaka H, Fujimiya M, Kashiwagi A, Kikkawa R. Increased intestinal glucose absorption and postprandial hyperglycaemia at the early step of glucose intolerance in Otsuka Long-Evans Tokushima Fatty rats. *Diabetologia*. 1998;41(12):1459–1466. https://doi.org/10.1007/s001250051092.
7. Dyer J, Wood IS, Palejwala A, Ellis A, Shirazi-Beechey SP. Expression of monosaccharide transporters in intestine of diabetic humans. *Am J Physiol Gastrointest Liver Physiol*. 2002;282(2):G241–G248. https://doi.org/10.1152/ajpgi.00310.2001.
8. Marks J, Carvou NJ, Debnam ES, Srai SK, Unwin RJ. Diabetes increases facilitative glucose uptake and GLUT2 expression at the rat proximal tubule brush border membrane. *J Physiol*. 2003;553(Pt 1):137–145. https://doi.org/10.1113/jphysiol.2003.046268.
9. Bhavadharini B, Mohan V, Dehghan M, et al. White rice intake and incident diabetes: a study of 132,373 participants in 21 countries. *Diabetes Care*. 2020;43(11):2643–2650. https://doi.org/10.2337/dc19-2335.
10. Song S, Young Paik H, Song WO, Song Y. Metabolic syndrome risk factors are associated with white rice intake in Korean adolescent girls and boys. *Br J Nutr*. 2015;113(3):479–487. https://doi.org/10.1017/S0007114514003845.
11. Friedman M. Rice brans, rice bran oils, and rice hulls: composition, food and industrial uses, and bioactivities in humans, animals, and cells. *J Agric Food Chem*. 2013;61(45):10626–10641. https://doi.org/10.1021/jf403635v.
12. Shao Y, Bao J. Polyphenols in whole rice grain: genetic diversity and health benefits. *Food Chem*. 2015;180:86–97. https://doi.org/10.1016/j.foodchem.2015.02.027.
13. Surarit W, Jansom C, Lerdvuthisopon N, Kongkham S, Hansakul P. Evaluation of antioxidant activities and phenolic subtype contents of ethanolic bran extracts of Thai pigmented rice varieties through chemical and cellular assays. *Int J Food Sci Technol*. 2015;50:990–998.
14. Munkong N, Thim-Uam A, Pengnet S, et al. Effects of red rice bran extract on high-fat diet-induced obesity and insulin resistance in mice. *Prev Nutr Food Sci*. 2022;27(2):180–187. https://doi.org/10.3746/pnf.2022.27.2.180.
15. Munkong N, Lonan P, Mueangchang W, Yadyookai N, Kanjoo V, Yoysungnoen B. Red rice bran extract attenuates adipogenesis and inflammation on white adipose tissues in high-fat diet-induced obese mice. *Foods*. 2022;11(13). https://doi.org/10.3390/foods11131865.
16. Limtrakul P, Yodkeeree S, Pitchakarn P, Punfa W. Anti-inflammatory effects of proanthocyanidin-rich red rice extract via suppression of MAPK, AP-1 and NF-κB pathways in Raw 264.7 macrophages. *Nutr Res Prac*. 2016;10(3):251–258. https://doi.org/10.4162/nrp.2016.10.3.251.
17. Pintha K, Yodkeeree S, Limtrakul P. Proanthocyanidin in red rice inhibits MDA-MB-231 breast cancer cell invasion via the expression control of invasive proteins. *Biol Pharm Bull*. 2015;38(4):571–581. https://doi.org/10.1248/bpb.b14-00719.
18. Pintha K, Yodkeeree S, Pitchakarn P, Limtrakul P. Anti-invasive activity against cancer cells of phytochemicals in red jasmine rice (Oryza sativa L.). *Asian Pac J Cancer Prev APJCP*. 2014;15(11):4601–4607. https://doi.org/10.7314/apjcp.2014.15.11.4601.
19. Boue SM, Daigle KW, Chen MH, Cao H, Heiman ML. Antidiabetic potential of purple and red rice (oryza sativa L.) bran extracts. *J Agric Food Chem*. 2016;64(26):5345–5353. https://doi.org/10.1021/acs.jafc.6b01909.
20. Murthy P, Manjunatha M, Sulochannama G, Naidu M. Extraction, characterization and bioactivity of coffee anthocyanins. *Eur J Biol*. 2012;4(1):13–19.
21. Price ML, Van Scoyoc S, Butler LG. A critical evaluation of the vanillin reaction as an assay for tannin in sorghum grain. *J Agric Food Chem*. 1978;26(5):1214–1218.
22. Fajardo RJ, Karim L, Calley VI, Bouxsein ML. A review of rodent models of type 2 diabetic skeletal fragility. *J Bone Miner Res*. 2014;29(5):1025–1040. https://doi.org/10.1002/jbmr.2210.
23. Wallace TM, Levy JC, Matthews DR. Use and abuse of HOMA modeling. *Diabetes Care*. 2004;27(6):1487–1495. https://doi.org/10.2337/diacare.27.6.1487.
24. Tervaert TW, Mooyaart AL, Amann K, et al. Pathologic classification of diabetic nephropathy. *J Am Soc Nephrol*. 2010;21(4):556–563. https://doi.org/10.1681/ASN.2010010010.
25. Yoon EJ, Seong HR, Kyung J, et al. Stamina-enhancing effects of human adipose-derived stem cells. *Cell Transplant*. 2021;30, 9636897211035409. https://doi.org/10.1177/09636897211035409.
26. Reagan-Shaw S, Nihal M, Ahmad N. Dose translation from animal to human studies revisited. *Faseb J*. 2008;22(3):659–661. https://doi.org/10.1096/fj.07-9574LSF.
27. Bettaieb A, Vazquez Prieto MA, Rodriguez Lanzi C, et al. (-)-Epicatechin mitigates high-fructose-associated insulin resistance by modulating redox signaling and endoplasmic reticulum stress. *Free Radic Biol Med*. 2014;72:247–256. https://doi.org/10.1016/j.freeradbiomed.2014.04.011.
28. Hubac M, Strelka F, Borský I, Hubacová L. Application of the relative summary climatic indices during work in heat for ergonomic purposes. *Ergonomics*. 1989;32(7):733–750. https://doi.org/10.1080/00140138908966839.
29. Ormazabal P, Scazzocchio B, Varì R, et al. Effect of protocatechuic acid on insulin responsiveness and inflammation in visceral adipose tissue from obese individuals:

possible role for PTP1B. *Int J Obes*. 2018;42(12):2012–2021. https://doi.org/10.1038/s41366-018-0075-4.
30. Wu T, Rayner CK, Jones KL, Xie C, Marathe C, Horowitz M. Role of intestinal glucose absorption in glucose tolerance. *Curr Opin Pharmacol*. 2020;55:116–124. https://doi.org/10.1016/j.coph.2020.10.017.
31. Merino B, Fernández-Díaz CM, Cózar-Castellano I, Perdomo G. Intestinal fructose and glucose metabolism in health and disease. *Nutrients*. 2019;12(1). https://doi.org/10.3390/nu12010094.
32. Kellett GL, Brot-Laroche E. Apical GLUT2: a major pathway of intestinal sugar absorption. *Diabetes*. 2005;54(10):3056–3062. https://doi.org/10.2337/diabetes.54.10.3056.
33. Sato S, Takeo J, Aoyama C, Kawahara H. Na+-glucose cotransporter (SGLT) inhibitory flavonoids from the roots of Sophora flavescens. *Bioorg Med Chem*. 2007;15(10):3445–3449. https://doi.org/10.1016/j.bmc.2007.03.011.
34. Li Q, Wang C, Liu F, et al. Mulberry leaf polyphenols attenuated postprandial glucose absorption via inhibition of disaccharidases activity and glucose transport in Caco-2 cells. *Food Funct*. 2020;11(2):1835–1844. https://doi.org/10.1039/c9fo01345h.
35. Shimizu M, Kobayashi Y, Suzuki M, Satsu H, Miyamoto Y. Regulation of intestinal glucose transport by tea catechins. *Biofactors*. 2000;13(1-4):61–65. https://doi.org/10.1002/biof.5520130111.
36. Kobayashi Y, Suzuki M, Satsu H, et al. Green tea polyphenols inhibit the sodium-dependent glucose transporter of intestinal epithelial cells by a competitive mechanism. *J Agric Food Chem*. 2000;48(11):5618–5623. https://doi.org/10.1021/jf0006832.
37. Walker J, Jijon HB, Diaz H, Salehi P, Churchill T, Madsen KL. 5-aminoimidazole-4-carboxamide riboside (AICAR) enhances GLUT2-dependent jejunal glucose transport: a possible role for AMPK. *Biochem J*. 2005;385(Pt 2):485–491. https://doi.org/10.1042/BJ20040694.
38. Tang X, Xiong K. Epidermal growth factor activates EGFR/AMPK signalling to up-regulate the expression of SGLT1 and GLUT2 to promote intestinal glucose absorption in lipopolysaccharide challenged IPEC-J2 cells and piglets. *Ital J Anim Sci*. 2020;21(1):943–954.
39. Ontawong A, Duangjai A, Srimaroeng C. Bean extract inhibits glucose transport and disaccharidase activity in Caco-2 cells. *Biomed Rep*. 2021;15(3):73. https://doi.org/10.3892/br.2021.1449.
40. Balakrishnan A, Stearns AT, Rhoads DB, Ashley SW, Tavakkolizadeh A. Defining the transcriptional regulation of the intestinal sodium-glucose cotransporter using RNA-interference mediated gene silencing. *Surgery*. 2008;144(2):168–173. https://doi.org/10.1016/j.surg.2008.03.010.
41. Párrizas M, Maestro MA, Boj SF, et al. Hepatic nuclear factor 1-alpha directs nucleosomal hyperacetylation to its tissue-specific transcriptional targets. *Mol Cell Biol*. 2001;21(9):3234–3243. https://doi.org/10.1128/MCB.21.9.3234-3243.2001.
42. Drozdowski LA, Thomson AB. Intestinal sugar transport. *World J Gastroenterol*. 2006;12(11):1657–1670. https://doi.org/10.3748/wjg.v12.i11.1657.
43. Kanungo S, Wells K, Tribett T, El-Gharbawy A. Glycogen metabolism and glycogen storage disorders. *Ann Transl Med*. 2018;6(24):474. https://doi.org/10.21037/atm.2018.10.59.
44. Macauley M, Smith FE, Thelwall PE, Hollingsworth KG, Taylor R. Diurnal variation in skeletal muscle and liver glycogen in humans with normal health and Type 2 diabetes. *Clin Sci (Lond)*. 2015;128(10):707–713. https://doi.org/10.1042/CS20140681.
45. Ashcroft FM, Rohm M, Clark A, Brereton MF. Is type 2 diabetes a glycogen storage disease of pancreatic β cells? *Cell Metabol*. 2017;26(1):17–23. https://doi.org/10.1016/j.cmet.2017.05.014.
46. Ceperuelo-Mallafré V, Ejarque M, Serena C, et al. Adipose tissue glycogen accumulation is associated with obesity-linked inflammation in humans. *Mol Metabol*. 2016;5(1):5–18. https://doi.org/10.1016/j.molmet.2015.10.001.
47. Barthel A, Schmoll D. Novel concepts in insulin regulation of hepatic gluconeogenesis. *Am J Physiol Endocrinol Metab*. 2003;285(4):E685–E692. https://doi.org/10.1152/ajpendo.00253.2003.
48. Sutherland C, O'Brien RM, Granner DK. New connections in the regulation of PEPCK gene expression by insulin. *Philos Trans R Soc Lond B Biol Sci*. 1996;351(1336):191–199. https://doi.org/10.1098/rstb.1996.0016.
49. Lin CH, Wu JB, Jian JY, Shih CC. (-)-Epicatechin-3-O-β-D-allopyranoside from Davallia formosana prevents diabetes and dyslipidemia in streptozotocin-induced diabetic mice. *PLoS One*. 2017;12(3), e0173984. https://doi.org/10.1371/journal.pone.0173984.
50. El-Sonbaty YA, Suddek GM, Megahed N, Gameil NM. Protocatechuic acid exhibits hepatoprotective, vasculoprotective, antioxidant and insulin-like effects in dexamethasone-induced insulin-resistant rats. *Biochimie*. 2019;167:119–134. https://doi.org/10.1016/j.biochi.2019.09.011.